PCCP

ROYAL SOCIETY OF CHEMISTRY

PAPER

View Article Online
View Journal | View Issue

Cite this: *Phys. Chem. Chem. Phys.*, 2021, **23**, 1706

Unravelling the nature of citric acid: L-arginine:water mixtures: the bifunctional role of water†

Ana Roda, [a] Filipa Santos, [a] Yeong Zen Chua, [b] Aarti Kumar, [c] Hoang Tam Do, [c] Alexandre Paiva, [a] Ana Rita C. Duarte [a] and Christoph Held *[c]

The use of water as a component of deep eutectic systems (DES) has raised some questions regarding its influence on the nature of the mixture. Does it form a DES or an aqueous solution and what is the role of water? In this work, the nature of citric acid:L-arginine:water mixtures was explored through phase equilibria studies and spectroscopic analysis. In a first step, PC-SAFT was validated as a predictive tool to model the water influence on the solid liquid equilibria (SLE) of the DES reline using the individual-component approach. Hence, activity coefficients in the ternary systems citric acid:L-arginine:water and respective binary combinations were studied and compared using ePC-SAFT. It was observed that the water-free mixtures citric acid:L-arginine showed positive deviation from Raoult's law, while upon addition of water strong negative deviation from Raoult's law was found, yielding melting depressions around 100 K. Besides these strong interactions, pH was found to become acidic (pH = 3.5) upon water addition, which yields the formation of charged species ($[H_2Cit]^-$ and [L-arg]$^+$). Thus, the increased interactions between the molecules upon water addition might be caused by several mechanisms such as hydrogen bonding or ionic forces, both being induced by water. For further investigation, the liquid mixtures citric acid:L-arginine:water were studied by FTIR and NMR spectroscopy. FTIR spectra disproved a possible solubility enhancement caused by salt formation between citric acid and L-arginine, while NMR spectra supported the formation of a hydrogen bonding network different from the binary systems citric acid:water and L-arginine:water. Either being a DES or other type of non-ideal solution, the liquefaction of the studied systems is certainly caused by a water-mediator effect based on the formation of charged species and cross interactions between the mixture constituents.

Received 21st September 2020,
Accepted 27th December 2020

DOI: 10.1039/d0cp04992a

rsc.li/pccp

Introduction

First defined by Abbott,[1] deep eutectic solvents/systems (DES) are commonly described as mixtures of two or more components. The hydrogen-bonding interactions lead to the formation of a liquid with a lower freezing/melting temperature than the pure constituents.[2–5] This concept was also expanded for mixtures with glass transition temperatures instead of melting points, being called Low-Transition-Temperature-Mixtures (LTTMs).[6] They have emerged as highly promising systems to be used in several applications due to their versatility and potentially green and sustainable character.[2–6]

Water is recognized as a universal solvent due to its ability in establishing hydrogen-bonding interactions with the solute. In fact "no other molecule has the hydrogen-bonding potential of water".[7] Due to this strong capacity in forming hydrogen bonds, either as hydrogen-bond acceptor or donor, the influence of water on the development of new solvent classes, as the DES, has been explored. Ackhar and co-workers presented a review summarizing some of the studies involving the influence of water in DES, up to 2018. Most of the works reported similar conclusions. Overall, the addition of water to DES up to 50 wt% maintained their original intermolecular network, even after incorporation of water hydrogen-bonds.[8] However, above certain amounts, water can solvate the isolated compounds, disrupting

[a] *LAQV, REQUIMTE, Departamento de Química da Faculdade de Ciências e Tecnologia, Universidade Nova de Lisboa, 2829-516 Caparica, Portugal. E-mail: a.roda@fct.unl.pt, mfca.santos@campus.fct.unl.pt, alexandre.paiva@fct.unl.pt, aduarte@fct.unl.pt*
[b] *Institute of Physics, University of Rostock, Albert-Einstein-Str. 23-24, 18051 Rostock, Germany*
[c] *Laboratory of Thermodynamics, Department of Biochemical and Chemical Engineering, TU Dortmund, 44227 Dortmund, Germany. E-mail: christoph.held@tu-dortmund.de*

† Electronic supplementary information (ESI) available. See DOI: 10.1039/d0cp04992a

the DES supramolecular complex and forming an aqueous solution.[8–12] More recent studies also support these findings and further suggest the formation of water-based DES, accompanied by a much deeper melting depression upon water addition compared to the water-free systems.[13,14] While these studies are all based on choline chloride-based DES, they highlight the importance of characterizing the water influence on other DES, opening the possibility to include water in the DES preparation as a starting material rather than a solvent.

Recently, mixtures of citric acid : L-arginine : water of mole ratios 1 : 1 : 4, 1 : 1 : 5, 1 : 1 : 6, 1 : 1 : 7, 2 : 1 : 7, 2 : 1 : 8, 2 : 1 : 9 were reported as new DES,[15,16] given their low water amounts, between 15 to 25 weight percent. Although the authors named these mixtures as DES, given the complexity of these systems and the presence of water, other possibilities may be considered. Is the water acting as a solvent, forming a regular aqueous solution? Are the citric acid and L-arginine forming a salt? The nature of these mixtures was explored by state-of-the-art parameters commonly used to define thermodynamic properties and the intermolecular interactions of the DESs.[17]

In this regard, solid–liquid equilibria (SLE) studies are an important tool as they can provide information about the composition, temperature range and intermolecular interactions responsible for the solid–liquid phase transitions. Namely, the melting temperatures and the activity coefficients of a certain mixture allow to evaluate if they present a negative deviation from ideality (Raout's law).[18–21] From this, the activity coefficients translate the cross-interactions affinity between the constituents of the mixture, evaluating their 'predisposition' to cross-interact. Perturbed-Chain Statistical Associating Fluid Theory (PC-SAFT) is an equation-of-state-based model that can be applied in modelling the SLE of mixtures considering hard-chain fluids as a reference.[18–22] In addition to the short-range interactions considered in PC-SAFT, electrolyte PC-SAFT (ePC-SAFT) is a variant that also accounts for long-range interactions promoted by charged species.[23] Further, PC-SAFT was considered to be highly accurate in a recent review comparing several thermodynamic modelling techniques.[22]

Beyond the thermodynamic properties, the establishment and type of intermolecular interactions responsible for the liquefaction of these mixtures must be addressed. Fourier transform infrared (FTIR) and nuclear magnetic resonance (NMR) spectroscopy are commonly used for this purpose. FTIR spectroscopy identifies the molecular functional groups of the involved species by specific vibrational frequencies defined by their dipole moment. Further, FTIR can be used to detect intermolecular interactions because they change the dipole moments of the involved functional groups, shifting the respective signals in the FTIR spectra.[17,24,25] NMR spectroscopy can be used to identify hydrogen bonding interactions or modifications through shifts in proton NMR spectra.[26–28] Additionally, information regarding intermolecular and spatial correlations can be obtained through two-dimensional nuclear Overhauser effect spectroscopy (2D NOESY) analysis.[26]

In the present work we characterized the SLE and other physicochemical properties of the ternary system citric acid:L-arginine:water through the introduced techniques while presenting some limitations of these tools towards distinction between a DES from a regular solution.

Experimental

Chemicals

Citric acid monohydrate [5949-29-1] (≥99.5% purity) was purchased from PanReac AppliChem (Barcelona, Spain). L-Arginine [74-79-3] (≥98% purity) was acquired from Sigma Aldrich (St. Louis, MO, USA). The ternary mixtures of citric acid:L-arginine:water were prepared by heating and stirring, as described by Santos *et al.*[15] Deionized water was used for the preparation of these mixtures. Anhydrous high purity nitrogen was used for DSC measurements. Sodium hydroxide pellets (NaOH, >99% purity) [1310-73-2] and hydrochloric acid 37% (HCl) [7647-01-0] were bought from Normax-Chem (Marinha Grande, Portugal) and dimethyl sulfoxide-d_6 (DMSO-d_6, 99,96% D) [2206-27-1] from Eurisotop (St. Aubin, France).

Methods

Fast scanning calorimetry (FSC). The melting properties (T_m and $\Delta_m H$) of L-arginine were determined experimentally with a Fast Scanning Calorimeter (FSC) (Mettler Toledo Flash DSC1 equipped with thin film chip sensor UFS1), where the thermal decomposition before and during melting was avoided. The experimental FSC method of L-arginine is in accordance to the measurement strategy for other amino acids and dipeptides, where the detailed description of the experimental FSC method has been given previously.[29,30]

The crystallized sample L-arginine was heated with high scanning rates, β varying from 2000 K s^{-1} to 10000 K s^{-1} without sample degradation. The onset temperature of melting peak for scanning rates, $T_m(\beta)$, is shown in Fig. 1 (top), where the melting temperature of L-arginine was defined at zero heating rate, *i.e.* $T_{m,arg} = T_m(\beta \rightarrow 0)$, taking into consideration the thermal lag and possible super-heating.[31,32] Fig. 1 (bottom) shows the enthalpy ΔH of the melting peak of L-arginine with respect to sample mass, m_0. The melting enthalpy of L-arginine is denoted as the slope of the linear fit through zero, regardless of the scanning rates.[29,30,33,34] The experimentally determined melting properties of L-arginine in this work are summarized in Table 1.

Differential scanning calorimetry (DSC). The pure components and the ternary mixtures of citric acid:L-arginine:water were analysed through DSC.

DSC Q200 from TA Instruments Inc. was used to determine the melting temperature of citric acid. The sample was sealed in an aluminium hermetic pan/lid, and it was submitted to two cooling/heating cycles between 183 and 473 K, at a rate of 10 K min^{-1}, at a nitrogen at flow rate of 50 mL min^{-1}. The thermal analysis of the ternary mixture citric acid:L-arginine:water was made using the same method. The thermic events were acquired through the TA Universal Analysis 2000 (4.7.0.2) software.

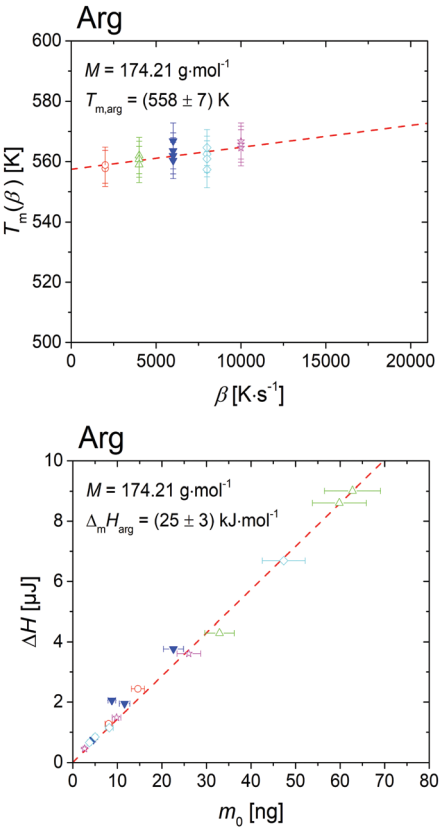

Fig. 1 (top) Extrapolated onset temperature of the melting peak of L-arginine (arg) as function of heating rate. The melting temperature at zero heating rate for arginine is $T_{m,arg}$ = (558 ± 7) K. (bottom) Enthalpy, ΔH of arginine in respect to initial sample.

Table 1 Melting temperature and enthalpy of the pure components used in this work

Compounds	T_m (K)	$\Delta_m H$ (kJ mol^{-1})	Ref.
Urea	405.8	13.61	35
ChCl	597	43.00	36
L-Arginine	558 ± 7	25 ± 3	This work
Citric acid	426.9	40.32[a]	This work[a] 37

[a] The T_m was obtained experimentally while $\Delta_m H$ was used from ref. 37.

Solid–liquid equilibrium modelling. The solid–liquid equilibrium of the mixtures was calculated through the thermodynamic simplified eqn (1):

$$x_i^L = \frac{1}{\gamma_i^L} \cdot \exp\left\{-\frac{\Delta_m H}{RT}\left(1 - \frac{T}{T_m}\right)\right\} \quad (1)$$

Eqn (1) allows calculating the solubility of the component i in the liquid phase x_i^L at specified temperature T, considering its activity coefficient γ_i^L, its melting enthalpy $\Delta_m H$ and its melting temperature T_m and the universal gas constant R (8.314 J mol^{-1} K^{-1}).

For the SLE modelling of the ternary mixtures reline:water and citric acid:L-arginine:water, eqn (1) was resolved to T, to predict the influence of water addition in the melting temperature of the ternary mixtures at fixed ratios of ChCl : urea (reline) or citric acid:L-arginine. The melting properties used in this work are summarized in Table 1.

PC-SAFT or ePC-SAFT was applied for the determination of the activity coefficients (γ_i), using the following equations:

$$\gamma_i = \frac{\varphi_i}{\varphi_{0i}} \quad (2)$$

$$\ln \varphi_i = \frac{\mu_i^{res}}{RT} - \ln(Z) \quad (3)$$

where φ_{0i} and φ_i represent the fugacity coefficients of the pure compound and of the component i in the mixture, respectively; μ_i^{res} is the residual chemical potential of compound i and Z the compressibility factor. Z and μ_i^{res} were derived from residual Helmholtz energy, a^{res}:

$$a^{res} = a^{hc} + a^{disp} + a^{assoc} + a^{ion} \quad (4)$$

which considers the contribution of hard-chain fluid (a^{hc}), dispersive (a^{dis}), associative (a^{assoc}) and ionic interactions (a^{ion}). The determination of these interactions required PC-SAFT parameters of the pure components; all the pure-component parameters were available from literature and are listed in Table 3. To describe mixtures, Berthelot–Lorenz combining rules and Wolbach–Sandler mixing rules were applied among all components. Binary parameters were applied in this work according to eqn (5):

$$k_{ij} = k_{ij}^a + k_{ij}^T \quad (T - 298.15\ \text{K}) \quad (5)$$

The binary parameters used in this work are listed in Table 4. All k_{ij} parameters are temperature independent, except for the binary ChCl:water. The k_{ij} used for the binary L-arginine:water was fitted to the isoelectric point region[38] but a different k_{ij} was required to describe correctly the interactions between [L-arginine]$^+$ and water at pH 3.5. This was performed according to previous works by solving dissociation equilibria and solubility.[39–41]

pH measurements. The pH of liquid mixtures was measured using an analogic pH meter (914 pH/Conductometer, model 2.914.0220, Metrohm), with a glass electrode coupled to a temperature sensor (NTC) (6.0228.010, Metrohm). All measurements were performed at room temperature.

Fourier transform infrared spectroscopy. FTIR spectra was recorded on a PerkinElmer Spectrum Two (Waltham, MA, USA) with attenuated total reflection (ATR) in the Transmittance mode and in a wavenumber range of 400–4000 cm^{-1}.

Nuclear magnetic resonance. Proton nuclear magnetic resonance (^{1}H NMR) and 2D NOESY spectra were recorded on a Bruker Avance III 400 spectrometer at 400 MHz. Spectra were obtained from about 400 μL of each sample with 50 μL of DMSO-d$_6$. Chemical shifts are expressed in ppm. MestReNova software (11.0.4-18998) was used for data analysis.

Results and discussion

Solid–liquid equilibria

FSC. The melting properties of L-arginine are required to apply eqn (1). In the literature, some attempts have been made to determine its melting properties;[15,42] however, due to its early degradation,[43] it was not possible to determine accurate values. In this work, the melting properties of L-arginine were determined for the first time directly with FSC as $T_m = (558 \pm 7)$ K; $\Delta_m H = (25 \pm 3)$ kJ mol^{-1}. This is only possible as FSC allows the sample to reach the melting temperature with high heating rate, without the thermal decomposition before and during melting.

DSC. The melting properties determined in this work for the pure components citric acid and L-arginine are summarized in Table 1. The T_m obtained for citric acid (426.9 K) is in accordance with data previously reported in literature by Meltzer *et al.* (427.80 ± 0.09 K)[37] and Wilhoit *et al.* (426.05–428.15 K).[44]

Regarding the ternary mixtures of citric acid : L-arginine : water, thermal events were acquired for ratios between 1 : 1 : 7 and 1 : 1 : 4 (molar). The mixtures have glass transition temperatures (T_g) ranging from 217 to 238 K, respectively.

Moreover, the mixtures with higher water content (1 : 1 : 7 and 1 : 1 : 6) were found to have melting peaks of around 260 K. This phenomenon did not occur for the mixtures with lower water content (1 : 1 : 5 and 1 : 1 : 4).

Within the studied range of temperature and molar ratios, no other thermal events were detected. Since no experimental T_m values for the ternary mixtures could be obtained, it is not possible to apply a thermodynamic correlation model (*e.g.* common activity coefficient models) for SLE modelling. Thus, eqn (1) requires a predictive model for the determination of activity coefficients. PC-SAFT was used for this purpose. As quantitative validation is impossible for citric acid:L-arginine:water, in a first step the SLE for reline:water was predicted, for which experimental data is available in literature.[45]

PC-SAFT validation for reline:water. The impact of water addition on the melting temperature (T_m) of reline, the eutectic composition of choline chloride (ChCl) and urea (1 : 2 molar ratio), was experimentally studied by Meng *et al.*[45] In the present work, PC-SAFT was used to model the SLE using the individual-component approach; that is, the three components ChCl:urea:water were explicitly considered for modelling. The pure-component parameters are available in the literature, see Table 3. One binary parameter between ChCl and urea was fitted in this work to match the composition of reline at the eutectic temperature, listed in Table 4. As observed in Fig. 2, PC-SAFT allows quantitatively predicting the decrease in the melting temperature (ΔT) of reline upon addition of water; the result is called 'prediction' as no parameter was adjusted to the experimental data of the ternary mixture ChCl:urea:water. This validates the use of PC-SAFT to predict the influence of water on melting temperatures. Thus, the individual-component approach within PC-SAFT is a powerful approach to predict SLE for systems that lack experimental data, such as for citric acid:L-arginine:water.

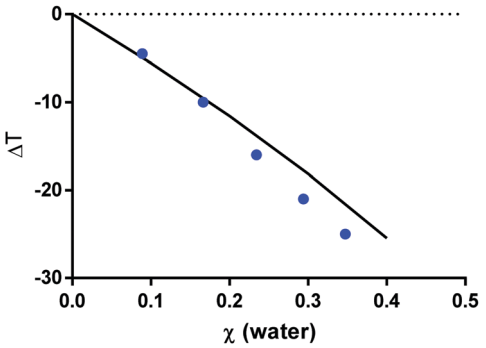

Fig. 2 Decrease of the melting temperature at the eutectic composition of reline upon water addition. Symbols correspond to experimental data[45] while the line corresponds to the PC-SAFT prediction results using the melting properties from Table 1 and the PC-SAFT parameters from Tables 2 and 3. $\Delta T = 0$ correspond to the binary mixture without water.

PC-SAFT modelling for citric acid:L-arginine:water. Prior to the study of the ternary mixture citric acid:L-arginine:water, the binary combinations of the three components were investigated. In Fig. 3, it can be observed that the solubility of L-arginine in water can be predicted accurately using PC-SAFT parameters for the pure components from the literature and the new letting properties from FSC. These parameters were not fitted to solubility data; nevertheless, the comparison between the PC-SAFT predictions and the experimental data regarding L-arginine solubility in water[46] is outstanding. Further, PC-SAFT allowed accurately modelling the literature data for the solubility of citric acid in water[47,48] (Fig. 3) using one binary k_{ij} parameter as listed in Table 4. The k_{ij} was adjusted to solubility data above 310 K, as below this temperature citric acid crystallizes as hydrate.

The SLE of the binary mixture citric acid:L-arginine was predicted with PC-SAFT using the parameters from Table 3 and the results are shown in Fig. 4. A qualitatively similar phase behaviour to the mixture L-arginine:water can be observed for citric acid:L-arginine, translating the low solubility of L-arginine in both, citric acid and water. From these, the predicted eutectic point of the mixture citric acid:L-arginine (χ(citric acid) ~ 0.96 with a T_m ~ 425.4 K) is almost equivalent to T_m of pure citric acid (426.9 K). Moreover, the values of the activity coefficients of citric acid and L-arginine in this mixture are

Table 2 Summary of the mixtures prepared with citric acid, L-arginine and H_2O, their ratio, physical state and pH

Mixture	Molar ratio	Physical state	pH
Citric acid : L-arginine : H_2O	0.1 : 1 : 7	White solid paste	—
Citric acid : L-arginine : H_2O	0.2 : 1 : 7	White solid paste	—
Citric acid : L-arginine : H_2O	0.5 : 1 : 7	Translucid liquid	4.76
Citric acid : L-arginine : H_2O	1 : 1 : 7	Translucid liquid	3.58 ± 0.15
Citric acid : H_2O	1 : 7	Translucid liquid	0.46
Citric acid : H_2O pH 3.5	1 : 7	White solid paste	—
Citric acid : H_2O pH 3.5	—[a]	Translucid liquid	3.62
L-Arginine : H_2O	1 : 7	White solid paste	—
L-Arginine : H_2O pH 3.5	—[b]	Translucid liquid	3.43

[a] Diluted with H_2O until a translucid liquid was obtained. [b] Diluted with water and HCl until a translucid liquid at pH around 3.5 was obtained.

Table 3 Pure-component parameters used for PC-SAFT modelling. The pure-component parameters of ChCl, urea, and L-arginine were fitted to experimental data of their aqueous solutions in the mentioned references by using the pure-component parameters of water as listed here. Thus, such parameters are not independent of each other; this explains the use of these parameters without further considering changes or improvements within this manuscript

Compound	σ_i (Å)	u_i/k_B	m_i^{seg}	$\varepsilon^{A_iB_i}/k_B$	$k^{A_iB_i}$	N_{HBD}/N_{HBA}	Ref.
Urea	2.4456	368.2302	4.244115	3068.31	0.0010	1/1	35
ChCl	2.3678	228.0702	13.01519	8000.00	0.2000	1/1	66
Water	2.7927[a]	353.9449	1.204659	2425.67	0.04509	1/1	67
L-Arginine[b]	2.6572	349.7065	9.90818	2555.45	0.03926	3/1	38
Citric acid[b]	2.7230	227.1800	8.54600	2488.00	0.04400	4/4	20

[a] Temperature-dependent segment diameter used according to ref. 67. [b] Pure-component parameters of their charged species set equal to the neutral molecules.

Table 4 Binary parameters applied in PC-SAFT modelling

Binary pair	k_{ij}^a	k_{ij}^T	Ref.
Reline (ChCl:urea)	−0.045	—	This work
ChCl:water	−0.05838	0.0001	66
Urea:water	−0.0438	—	35
L-Arginine:water	−0.0145	—	38
[L-Arginine]$^+$:water	−0.045	—	This work
Citric acid:water	−0.11	—	This work
L-Arginine:citric acid	—	—	—

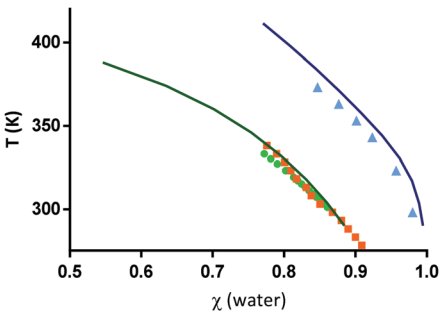

Fig. 3 Solubility data of L-arginine in water (triangles[46]) and of citric acid in water (squares;[47] circles[48]). Symbols correspond to experimental data while the lines correspond to PC-SAFT modelling results using the melting properties from Table 1 and the PC-SAFT parameters from Tables 2 and 3. χ represents the mole fraction.

greater than one (Fig. 6, χ(water) = 0), indicating rather weak attractive cross-interactions between citric acid and L-arginine. Besides, it presents a positive deviation from the ideal SLE calculations (blue dashed line), strengthening the lack of interactions between citric acid:L-arginine in a binary system.

The PC-SAFT prediction shown in Fig. 4 supports the fact that a DES is not formed between citric acid and L-arginine. Although experimental validation by DSC was not possible for this binary system, it can be reported that this mixture was prepared in the lab and it was found to be solid at room temperature. This scenario changes upon water addition.

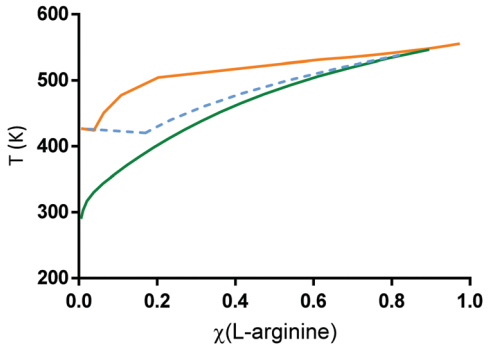

Fig. 4 PC-SAFT modelling of the SLE for the binary mixtures L-arginine:-water (green line) and L-arginine:citric acid (orange line) using the melting properties from Table 1 and the PC-SAFT parameters from Tables 2 and 3. The dashed blue line represents the ideal SLE of L-arginine:citric acid based on eqn (1).

As reported by Santos *et al.* and Roda *et al.*, ternary mixtures of citric acid:L-arginine:water at certain compositions are liquid at room temperature.[15,16] In the present work, the SLE of these mixtures was studied (Fig. 5).

The PC-SAFT predictions from Fig. 5 might not be quantitatively correct, since it was not possible to experimentally determine the T_m. Nevertheless, as the model showed to qualitatively predict the ΔT for reline upon water addition (Fig. 2), a qualitatively correct prediction of the SLE using PC-SAFT is expected also for modelling the water influence on the mixture of citric acid:L-arginine:water. Hence, PC-SAFT was used to model the ΔT of the system citric acid : L-arginine (at 1 : 1 molar composition) upon water addition. As observed in Fig. 5, there is a pronounced decrease of ΔT with water addition to the system citric acid : L-arginine. In comparison to the binary citric acid:L-arginine, there is a T_m reduction of about 100 K for the ternary mixture of citric acid : L-arginine : water 1 : 1 : 7 (molar, χ(water) = 0.78). This deep reduction in T_m could be compliable with the formation of a DES, but it might also be just the formation of a regular solution, which will be discussed in the following paragraphs.

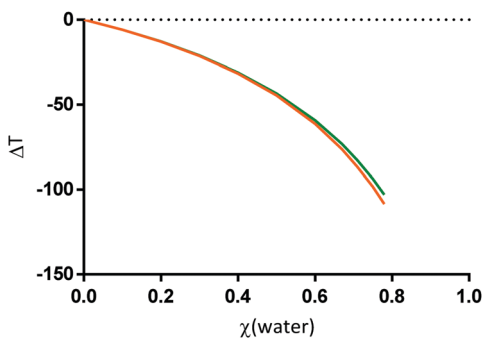

Fig. 5 PC-SAFT prediction of the influence of water on T_m (expressed as ΔT) upon water addition to the mixture citric acid : L-arginine 1 : 1 (molar), using the melting properties from Table 1 and the PC-SAFT parameters from Tables 2 and 3. Orange line: ΔT for the solubility of citric acid in the mixture; green line: ΔT for the solubility of L-arginine in the mixture. $\Delta T = 0$ corresponds to the binary mixture without water. Data from Table S1 (ESI†).

The PC-SAFT predictions shown in Fig. 3 and 5 (binary and ternary mixtures containing water, L-arginine, citric acid) assumed presence of only neutral species; charges were neglected, as application of eqn (1) requires that the same species are present in the solid or liquid state. However, the pH of the mixture and the pK_a of the molecules define their charge, which can deeply influence interactions and solubility behaviour. When both, L-arginine and citric acid are mixed with water, different pH values and thus, different species will occur. Fig. S1 (ESI†) shows the molecular species of citric acid or L-arginine expected to be present according to pH. Considering the case of the mixture citric acid : L-arginine : water 1 : 1 : 7 molar ratio, the measured pH was about 3.6 (Table 2). As observed in Fig. S1 (ESI†),[49] at this pH, the majority of L-arginine molecules will be positively charged, [L-arginine]$^+$; whereas for citric acid a mixture of the dehydrogenated form, [citrate]$^-$ and its neutral specie is expected. It is known that the solubility of citric acid is only slightly affected by pH changes (calculated using Advanced Chemistry Development (ACD/Labs) Software V11.02 (©1994–2020 ACD/Labs)). However, the solubility changes of L-arginine species from the isoelectric region (neutral species) to pH values between 2 and 9 ([L-arginine]$^+$) are more significant and must be considered to describe more realistically the interactions between [L-arginine]$^+$, water and citric acid at these pH values. This was accounted for by predicting activity coefficients by ePC-SAFT. The pure-component parameters of the charged species were inherited from the neutral molecules, and a k_{ij} for the binary [L-arginine]$^+$:water (Table 4) was adjusted according to previous works by solving dissociation equilibria and solubility.[39–41] For [citrate]:water the k_{ij} was considered to be the same as the neutral citric acid:water, given their similar behaviour in terms of solubility. The results are shown in Fig. 6–8. Activity coefficients equal to one correspond to an ideal behaviour while negative (or positive) deviations translate into a higher (or lower) interaction affinity between the constituents of the mixture, respectively.

As observed in Fig. 6 the activity coefficients of citric acid (γ_{cit}) in the ternary mixture gradually decrease upon water addition. The decrease from γ_{cit} = 1.51 to values lower than 1, namely for χ(water) = 0.78 with a γ_{cit} = 0.19, highly emphasizes

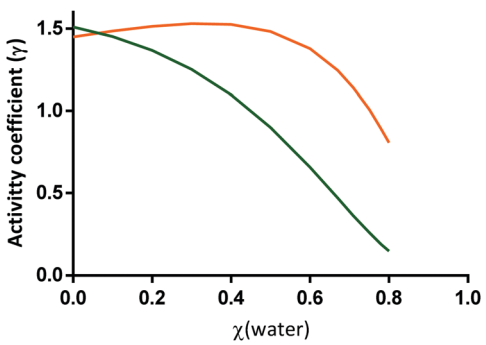

Fig. 6 Activity coefficients of citric acid (green line) and [L-arginine]$^+$ (orange line) when water is added to the mixture citric acid : L-arginine 1 : 1 (molar), predicted by ePC-SAFT using the parameters from Tables 2 and 3. Data from Table S2 (ESI†).

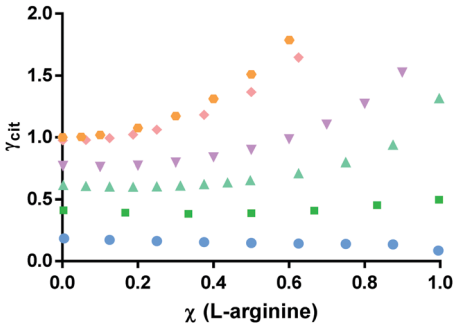

Fig. 7 Activity coefficients of citric acid in the mixture citric acid:L-arginine:water, at different relative molar fraction of L-arginine with respect to citric acid and constant water molar ratios. Circles: χ(water) = 0.8; squares: χ(water) = 0.7; triangles: χ(water) = 0.6; inverted triangles: χ(water) = 0.5; rhombi: χ(water) = 0.2; pentagons: χ(water) = 0.01. PC-SAFT results listed in Tables S3–S8 (ESI†).

the negative deviation of the mixture from Raoult's law. For [L-arginine]$^+$, a positive and almost constant deviation from ideality is observed for water molar ratios up to 0.71. Above this water content, the activity coefficient of [L-arginine]$^+$ (γ_{arg}^+) decreases pronouncedly, reaching negative deviation from Raoult's law when χ(water) $\geq$ 0.78. The lower γ_{cit} in comparison to γ_{arg}^+ indicates a higher contribution of citric acid to the melting depression of the mixture[50] and a higher affinity to establish cross-interactions in the mixture.

Until now, the results were discussed using a 1 : 1 molar ratio of citric acid : L-arginine. The influence of water on the T_m of the mixture might depend also on the ratio of citric acid:L-arginine. Thus, the activity coefficient of citric acid in the ternary mixture was also predicted for different L-arginine:citric acid ratios at constant water contents (Fig. 7).

Analysing the scenario where water is added to pure citric acid (χ(L-arginine) = 0), there is a decrease of γ_{cit} for increasing water amounts, with negative deviations from ideality ($\gamma_{cit} < 1$) when χ(water) $>$ 0.2. This situation is regularly explained by water solvation effect. It is also observed that, at low water content, the addition of L-arginine increases the activity coefficient of citric acid in the mixture, probably by inducing competition between species. This behavior is less noticeable as the χ(water) increases up to 0.6 and changes significantly for χ(water) $\geq$ 0.7. At this water amount or higher, the γ_{cit} seems to stabilize into an almost constant value for all the L-arginine ratios in the mixture. Further, an even more distinct behavior was observed for χ(water) = 0.8, where the addition of L-arginine seems to slightly favour the interactions of citric acid in the mixture. For that water content, the γ_{arg}^+ (Fig. 8) shows a positive deviation from Raoult's law for χ(L-arginine) $\leq$ 0.05, that shifts to a negative deviation from ideality, when χ(L-arginine) $\geq$ 0.1. This emphasizes that the addition of L-arginine to the mixture citric acid:L-arginine:water above a certain amount causes increased cross interactions, but only at high water content. This is a non-regular solution effect.

Interestingly, the mixtures of citric acid : L-arginine : water previously reported to be liquid (1 : 1 : 4, 1 : 1 : 5, 1 : 1 : 6, 1 : 1 : 7,

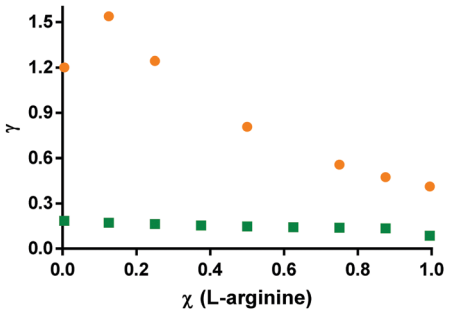

Fig. 8 Activity coefficients of [L-arginine]$^+$ (circles) and citric acid (squares) in the mixture citric acid:L-arginine:water, at a χ(water) = 0.8 and different relative molar ratios of L-arginine with respect to citric acid. PC-SAFT results listed in Tables S3 and S9 (ESI†).

2 : 1 : 7, 2 : 1 : 8, 2 : 1 : 9 mol ratios[15,16]) correspond to water molar contents between 0.7 and 0.8, which coincide within the range where this 'non-regular' behavior was detected. Moreover, the lowest γ_{cit} values predicted by the ePC-SAFT model and respective ratios, are in accordance with the formation of liquid phase mixtures at the ratios previously reported and herein explored.

Despite the possibility that the mixture citric acid:L-arginine:water might be a solution rather than a DES, the 'non-regular' behaviour observed for the activity coefficients within the only ratios reported to form a homogenous liquid phase has not yet been explained. It is certain that the liquid state is stabilized by water mediation, but also preponderantly influenced by the citric acid and L-arginine contents. Still, the type of network interactions responsible for this phenomenon are not known. Thus, from these data and the ePC-SAFT prediction alone it is not possible to postulate the type of mixture formed (DES, solution, salt), as different scenarios might fit the results presented.

Given the complexity of these systems and the impossibility to measure the SLE, spectroscopy analysis was additionally performed to further characterize the mixtures and to better understand their nature.

Physicochemical analysis

Aiming to complement the investigation on the nature of the mixtures citric acid:L-arginine:water, several binary and ternary mixtures involving these components were prepared for comparison and analysed through spectroscopic techniques. The mixture citric acid:L-arginine:water 1 : 1 : 7 (mol) was chosen as a model to compare with aqueous solutions of citric acid or L-arginine, in the same ratio or at the same pH (around 3.5) of the ternary mixture.

Furthermore, ternary mixtures with increasing citric acid molar ratio from 0.1 to 1 were prepared and analysed by FTIR; those that were liquid were also analysed by NMR in order to evaluate the role of citric acid in the mixture. The mixtures prepared, their ratios, physical state and pH are reported in Table 2.

From the ternary mixtures tested, it was observed that only the ones with citric acid molar ratios $\geq$0.5 formed translucid liquids, with pH $<$ 7. Since the pH alone might be the reason for the solubility increase of L-arginine in water, a mixture of the same ratio of L-arginine : water (1 : 7) was prepared and acidified with HCl rather than citric acid, to identify the role of pH. It was observed that this mixture did not lead to the formation of a liquid at room temperature, neither before nor after acidification. The other way around was also evaluated: changing the pH of the binary citric acid : water 1 : 7 (translucid liquid at pH 0.5) to pH = 3.5 using NaOH instead of L-arginine caused the formation of a white solid paste at room temperature. These observations support that the liquid formation is not only a function of pH, but it is additionally influenced by the involving species. In this case, the mixture of L-arginine and citric acid in the presence of water seems to have unique properties in addition to pH to promote their liquefaction. One possibility could be complexation of the oppositely charged species $[H_2Cit]^-$ and $[Arg]^+$ (Fig. S1, ESI†) in water yielding a salt that might have higher water solubility than the non-charged precursor molecules. Hence, this hypothesis was addressed in the following FTIR section.

FTIR. The functional groups of pure citric acid and L-arginine were identified, and the respective stretching and bending vibrations were assigned as summarized in Tables S11[51–55] and S12[51,56–58] (ESI†). The most important changes in the vibrations of the mixtures from Table 2 in comparison to the pure components are represented in the spectra of Fig. 9. Furthermore, the chemical structure of the pure components and their variation with pH is represented in Fig. S2 (ESI†). In the spectra of all mixtures under investigation, the water contribution can be identified by the broadening of the band regions between 3000–3500, 1500–1800 and 500–900 cm^{-1}. Nonetheless, it is possible to identify the peaks of L-arginine and citric acid. In the L-arginine powder form, two sharp peaks corresponding to the guanidine and primary amine groups can be distinguished at 3302 cm^{-1} and 3357 cm^{-1}, respectively. When water is added (L-arginine : water 1 : 7, Fig. 9b), a broader peak is observed for the guanidine amines due to their transition to the delocalized charge state. At pH 3.5 (Fig. 9c), the primary amine is also charged causing the amine peaks to overlap around 3323 cm^{-1}. Additionally, the O–H stretching of L-arginine in its pure form (3057 cm^{-1}, Fig. 9a) shifts to higher frequencies due to the establishment of hydrogen bonding interactions with the surrounding media (Fig. 9b–d). Regarding citric acid, the most important vibrations are from the O–H and C=O stretching of the carboxylic groups, centred at 3297 and 1719 cm^{-1}, respectively. When mixed with water at pH 3.5, the O–H vibrations are broadened and shifted, and the maximum is at 3340 cm^{-1}.

Comparing the citric acid : water and L-arginine : water mixtures at a pH = 3.5 with the ternary system of citric acid : L-arginine : water 1 : 1 : 7, it is possible to observe a combined contribution of the same O–H and N–H stretching peaks (Fig. 9c–e, dashed lines). This was also observed for the other analysed ratios of citric acid:L-arginine:water (Fig. S3, ESI†). If the liquids formed by the combination of citric acid, L-arginine and water were promoted by the ionic complexation of $[H_2Cit]^-$ and $[Arg]^+$, the dipole moments of those functional groups

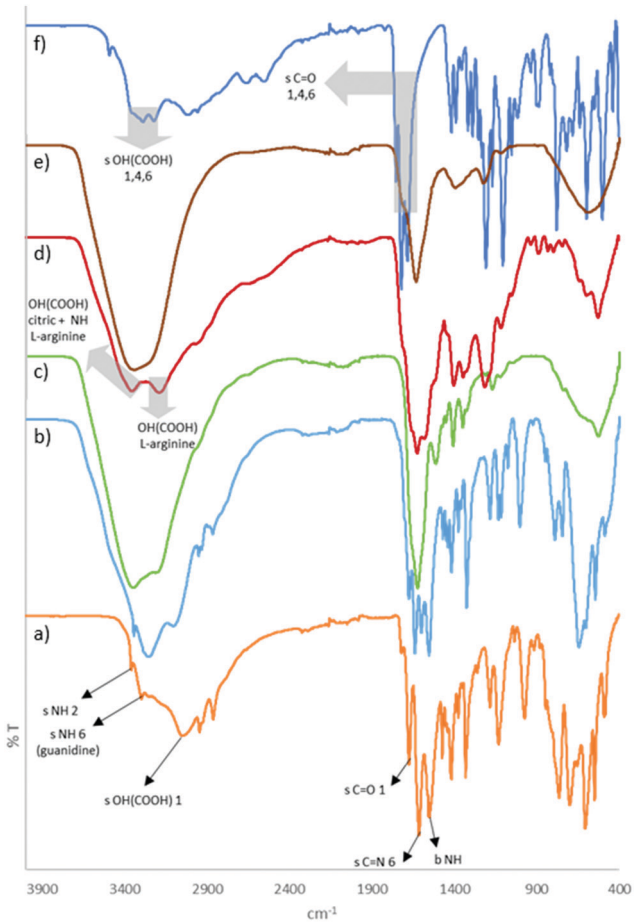

Fig. 9 FTIR spectra of (a) pure L-arginine (orange line); (b) L-arginine : H_2O 1 : 7 mol (light blue line); (c) L-arginine : H_2O pH = 3.5 (green line); (d) citric acid : L-arginine : H_2O 1 : 1 : 7 mol (red line); (e) citric acid : H_2O 1 : 7 mol (brown line); (f) pure citric acid (dark blue line). "s" and "b" refer to stretching and bending vibrations, respectively. Numbers attributed according to the chemical structures from Fig. S2 (ESI†).

would be changed. However, different vibrations in the FTIR spectra were not observed, refuting the salt formation hypothesis.

To sum up, the liquid is neither a case of salt formation nor exclusively induced by the acidic pH value. Thus, other L-arginine:-citric acid interactions mediated by water must be the reason for the deep melting point depression of the ternary system, probably H-bonding interactions. This was further explored by NMR analysis.

NMR. Aiming to investigate the nature of the mixtures citric acid:L-arginine:water, ^{1}H and NOESY NMR were performed. Only liquid mixtures were considered for comparison. In these context, the ^{1}H spectra for the aqueous solutions of the pure components at pH = 3.5 and the citric acid : water 1 : 7 mixture were compared with the ternary systems of citric acid : L-arginine : water 1 : 1 : 7 and 0.5 : 1 : 7 (Fig. 10).

For the system L-arginine:water at pH = 3.5, it was possible to identify the protons from water and most of the protons of the L-arginine's amine and alkyl groups (Fig. 10e); whereas for the citric acid : water at pH = 3.5 or at the molar ratio 1 : 7 it was only possible to detect the alkyl groups and a contribution of the OH-group protons overlapped with the protons from water. This influence of the OH group was attributed due to the downfield shift of the concentrated solution of citric acid (1 : 7 molar) (5.79 ppm, Fig. 10b) in comparison to its diluted solution at pH 3.5 (4.79 ppm, Fig. 10a). Interestingly, the same peak (5.79 ppm) appears in the case of the ternary mixture 1 : 1 : 7 (Fig. 10c), but it is broader. Further, it has a second peak at 5.20 ppm, also appearing in the ternary system 0.5 : 1 : 7. Given that the only difference from the samples of Fig. 10b to c was the addition of L-arginine, the appearance of a new peak is certainly caused by hydrogen-bonding interactions with the L-arginine molecules, in addition to the ones between citric acid and water. Regarding the broadening-effect observed for the ternary mixtures in comparison to the binary solutions, it might be related to the samples' high viscosity. According to Stokes–Einstein–Debye law, high viscosity mixtures lead to slower rotational molecular diffusion[59–62] and longer T_2 relaxation times.[63,64] These translate into broader NMR peaks, as previously reported for viscous DES mixtures.[65]

Moreover, in the NOESY spectra of the system citric acid : L-arginine : water 1 : 1 : 7 there are cross peaks between the protons from the citric acid alkyl groups and the protons of L-arginine chemical groups (Fig. 11) that may indicate spatial

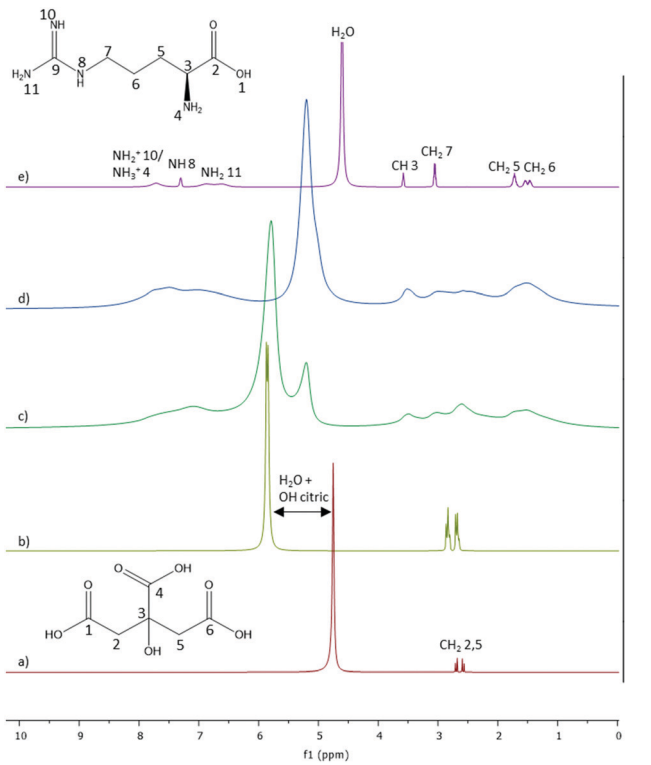

Fig. 10 ^{1}H NMR spectra of (a) citric acid : H_2O pH = 3.5; (b) citric acid : H_2O 1 : 7; (c) citric acid : L-arginine : H_2O 1 : 1 : 7; (d) citric acid : L-arginine : H_2O 0.5 : 1 : 7; (e) L-arginine : H_2O pH = 3.5. The functional groups of the protons detected were identified and numbers attributed according to the respective chemical structures (see species distribution in Fig. S2, ESI†).

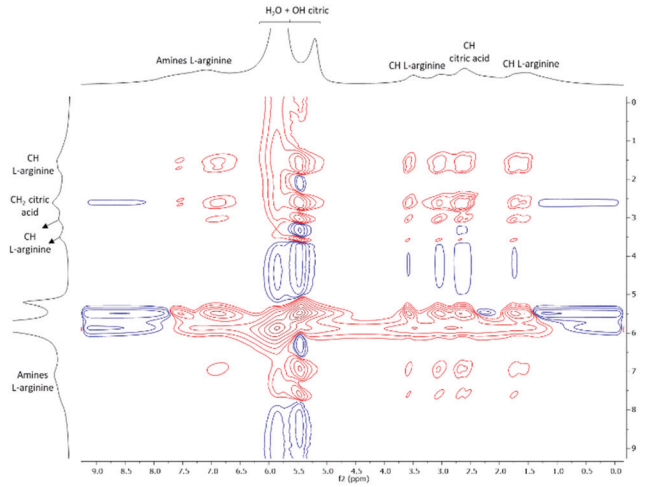

Fig. 11 2D NOESY spectra of the mixture citric acid : L-arginine : H_2O 1 : 1 : 7 mol. The functional groups of the protons identified are aligned with the respective peaks.

correlation. Similar correlations were observed for the mixture 0.5 : 1 : 7 (Fig. S4, ESI†). This may support that in addition to the expected interactions between H_2O–H_2O, citric acid–H_2O, citric acid–citric acid, L-arginine–H_2O and L-arginine–L-arginine, further citric acid–L-arginine and/or mutual interactions between the three components might occur. However, given that the cross peaks are in the same phase as the diagonal peaks (positive, red peaks), this might also be a case of spin diffusion due to the high viscosity. Still, since viscosity is a direct cause of mixing the three components, it is highly probable that they are spatially close and interacting. Combined with the evidence from ^{1}H NMR analysis that there is a change in the hydrogen bonding network when citric acid and L-arginine are mixed with water in comparison to their independent water solutions, these findings might be compliable with the formation of a supramolecular network, which is characteristic from DES. To properly address the interactions-network between the components that allowed to form the liquid ternary mixtures, dynamic molecular studies would have to be performed. Additionally, magic-angle spinning (MAS) NMR has recently been described as a good technique to overcome some of the conventional NMR limitations in the characterization of viscous mixtures, like DES.[65] This MAS NMR technique also allows to analyse and compare both liquid and solid mixtures, which, in the field of DES, might be highly useful in understanding those interactions between the involved molecules that are responsible for the mixture liquefaction.

Still, from our findings, it is noticeable that the interactions between the water molecules and the functional groups of citric acid and L-arginine, namely, amine, carboxyl and hydroxyl groups may play a major role in establishing those interactions.

Conclusions and final remarks

The ternary mixtures of citric acid:L-arginine:water previously reported in the literature as DES, have been questioned as whether or not they are regular solutions due to the water present in their composition. This work shows that these mixtures are prone to strong non-ideal behaviour induced by water addition. Water has a bifunctional role as it causes acidic environment (formation of charged species) and it acts as hydrogen-bonding mediator for the L-arginine and citric acid. As the phase behaviour depends on the ratio of the mixture's constituents, the thermodynamic model ePC-SAFT was used as a qualitative predictive model to predict the influence of water on the SLE. This prediction tool is particularly useful as it was not possible to obtain experimental SLE data for the system, due to decomposition, slow melting or to ultra-low melting points. Within this context, the influence of water on citric acid:L-arginine mixtures was studied in terms of SLE and activity coefficients. Novel melting properties of L-arginine were first determined through FSC, as this was required for SLE modelling. ePC-SAFT predicted a transition from positive to negative deviation from Raoult's law upon addition of water to citric acid:L-arginine at certain ratios. This rendered an estimated deep decrease in the T_m of these mixtures upon water addition as well as increased intermolecular interactions. Furthermore, the hypothesis of salt formation and pH influence to explain the deep decrease of T_m were explored. However, both could be contradicted (by pH control measurements without either citric acid or L-arginine and by the FTIR analysis). Finally, the formation of an altered hydrogen-bonding network was confirmed by NMR spectroscopy. The observed non-ideal behaviour of the mixture and the hydrogen-bonding formation in the mixture are consistent with (i) the hypothesis of DES formation and (ii) the occurrence of strong non-ideal solvation of the citric acid and L-arginine species in water. In this scenario (considering the high potential of water to establish hydrogen-bonding interactions) it is challenging to distinguish between non-ideal solvation and DES formation. Both phenomena are mainly promoted by hydrogen-bonding interactions between the constituents, causing a depression on the melting temperatures. To the best of our knowledge, the only difference reported in the literature that differentiates a DES from a regular solution is the structural network organization. Whereas DES are recognized by the supramolecular complexes formed between its constituents, aqueous solutions are considered when solvation of the isolated components occurs.[8–14] Thus, if distinguishable within the available state-of-the-art tools, this would only be possible by molecular dynamic simulations as activity-coefficient analyses rely on non-local spatially-averaged properties. Still, from the present work, important features of the ternary systems were characterized, and the crucial bifunctional role of water was postulated (formation of charged species and mediated hydrogen-bonded interactions between citric acid and L-arginine). Therefore, either a DES or a non-ideal aqueous solution, these ternary mixtures have new properties and might be considered as independent systems from conventional solvents.

In sum, it was shown that despite meeting the definition for a DES, still such definition is not sharp enough for complex aqueous mixtures and other liquid-based mixtures, as the current concepts of solvation and DES formation overlap.

For this reason, this work aims to instigate the scientific community in investing in the study of this type of mixtures while seeking for additional tools that may contribute to a comprehensive characterization and understanding of their nature.

Conflicts of interest

There are no conflicts to declare.

Acknowledgements

This project has received funding from the European Union's Horizon 2020 (European Research Council) under grant agreement no. ERC-2016-CoG 725034. This work was supported by the Associate Laboratory for Green Chemistry-LAQV which is financed by national funds from FCT/MCTES (UID/QUI/50006/2019). Further, C. H. and Y. Z. C. thank German Science Foundation (DFG) for funding (HE 7165/6-1 and CH 1922/1-1).

References

1 A. P. Abbott, G. Capper, D. L. Davies, R. K. Rasheed and V. Tambyrajah, Novel solvent properties of choline chloride/urea mixtures, *Chem. Commun.*, 2003, 70–71.
2 Q. Zhang, K. De Oliveira Vigier, S. Royer and F. Jérôme, Deep eutectic solvents: Syntheses, properties and applications, *Chem. Soc. Rev.*, 2012, **41**, 7108–7146.
3 A. Paiva, R. Craveiro, I. Aroso, M. Martins, R. L. Reis and A. R. C. Duarte, Natural deep eutectic solvents - Solvents for the 21st century, *ACS Sustainable Chem. Eng.*, 2014, **2**, 1063–1071.
4 E. L. Smith, A. P. Abbott and K. S. Ryder, Deep Eutectic Solvents (DESs) and Their Applications, *Chem. Rev.*, 2014, **114**, 11060–11082.
5 A. Paiva, A. A. Matias and A. R. C. Duarte, How do we drive deep eutectic systems towards an industrial reality ?, *Curr. Opin. Green Sustain. Chem.*, 2018, **11**, 81–85.
6 M. Francisco, A. Van Den Bruinhorst and M. C. Kroon, Low-transition-temperature mixtures (LTTMs): A new generation of designer solvents, *Angew. Chem., Int. Ed.*, 2013, **52**, 3074–3085.
7 D. L. Nelson and M. M. Cox, *Lehninger Principles of Biochemistry*, W. H. Freeman, New York, 7th edn, 2017.
8 T. El Achkar, S. Fourmentin and H. Greige-Gerges, Deep eutectic solvents: An overview on their interactions with water and biochemical compounds, *J. Mol. Liq.*, 2019, **288**, 111028.
9 Y. Dai, G.-J. Witkamp, R. Verpoorte and Y. H. Choi, Tailoring properties of natural deep eutectic solvents with water to facilitate their applications, *Food Chem.*, 2015, **187**, 14–19.
10 O. S. Hammond, D. T. Bowron and K. J. Edler, Effect of Water upon Deep Eutectic Solvent Nanostructure: An Unusual Transition from Ionic Mixture to Aqueous Solution, *Angew. Chem., Int. Ed.*, 2017, **56**, 9782–9785.
11 H. Passos, D. J. P. Tavares, A. M. Ferreira, M. G. Freire and J. A. P. Coutinho, Are Aqueous Biphasic Systems Composed of Deep Eutectic Solvents Ternary or Quaternary Systems ?, *ACS Sustainable Chem. Eng.*, 2016, **4**, 2881–2886.
12 J. Baz, C. Held, J. Pleiss and N. Hansen, Thermophysical properties of glyceline-water mixtures investigated by molecular modelling, *Phys. Chem. Chem. Phys.*, 2019, **21**, 6467–6476.
13 N. López-Salas, J. M. Vicent-Luna, S. Imberti, E. Posada, M. J. Roldán, J. A. Anta, S. R. G. Balestra, R. M. M. Castro, S. Calero, R. J. Jiménez-Riobóo, M. C. Gutiérrez, M. L. Ferrer and F. del Monte, Looking at the 'Water-in-Deep-Eutectic-Solvent' System: A Dilution Range for High Performance Eutectics, *ACS Sustainable Chem. Eng.*, 2019, **7**, 17565–17573.
14 L. Sapir and D. Harries, Restructuring a Deep Eutectic Solvent by Water: The Nanostructure of Hydrated Choline Chloride/Urea, *J. Chem. Theory Comput.*, 2020, **16**, 3335–3342.
15 F. Santos, M. I. P. S. Leitão and A. R. C. Duarte, Properties of Therapeutic Deep Eutectic Solvents of L-Arginine and Ethambutol for Tuberculosis Treatment, *Molecules*, 2018, **24**, 55.
16 A. Roda, F. Santos, A. A. Matias, A. Paiva and A. R. C. Duarte, Design and processing of drug delivery formulations of therapeutic deep eutectic systems for tuberculosis, *J. Supercrit. Fluids*, 2020, **161**, 104826.
17 G. Degam, Deep Eutectic Solvents Synthesis, *Characterization and Applications in Pretreatment of Lignocellulosic Biomass*, Electronic Theses and Dissertations, 2020, p. 1156.
18 P. V. A. Pontes, E. A. Crespo, M. A. R. Martins, L. P. Silva, C. M. S. S. Neves, G. J. Maximo, M. D. Hubinger, E. A. C. Batista, S. P. Pinho, J. A. P. Coutinho, G. Sadowski and C. Held, Measurement and PC-SAFT modeling of solid-liquid equilibrium of deep eutectic solvents of quaternary ammonium chlorides and carboxylic acids, *Fluid Phase Equilib.*, 2017, **448**, 69–80.
19 E. A. Crespo, L. P. Silva, A. R. Martins, L. Fernandez, J. Ortega, O. Ferreira, G. Sadowski, C. Held, S. P. Pinho and J. A. P. Coutinho, Characterization and Modeling of the Liquid Phase of Deep Eutectic Solvents Based on Fatty Acids/Alcohols and Choline Chloride, *Ind. Eng. Chem. Res.*, 2017, **56**, 12192–12202.
20 E. A. Crespo, L. P. Silva, M. A. R. Martins, M. Bülow, O. Ferreira, G. Sadowski, C. Held, S. P. Pinho and J. A. P. Coutinho, The Role of Polyfunctionality in the Formation of [Ch]Cl-Carboxylic Acid-Based Deep Eutectic Solvents, *Ind. Eng. Chem. Res.*, 2018, **57**, 11195–11209.
21 M. A. R. Martins, E. A. Crespo, P. V. A. Pontes, L. P. Silva, M. Bülow, G. J. Maximo, E. A. C. Batista, C. Held, S. P. Pinho and J. A. P. Coutinho, Tunable Hydrophobic Eutectic Solvents Based on Terpenes and Monocarboxylic Acids, *ACS Sustainable Chem. Eng.*, 2018, **6**, 8836–8846.
22 I. I. I. Alkhatib, D. Bahamon, F. Llovell, M. R. M. Abu-Zahra and L. F. Vega, Perspectives and guidelines on thermodynamic modelling of deep eutectic solvents, *J. Mol. Liq.*, 2020, **298**, 112183.

23 C. Held, T. Reschke, S. Mohammad, A. Luza and G. Sadowski, ePC-SAFT revised, *Chem. Eng. Res. Des.*, 2014, **92**, 2884–2897.
24 T. Aissaoui and I. M. AlNashef, Neoteric FT-IR Investigation on the Functional Groups of Phosphonium-Based Deep Eutectic Solvents, *Pharm. Anal. Acta*, 2015, **6**, 1–3.
25 H. Ghaedi, M. Ayoub, S. Sufian, B. Lal and Y. Uemura, Thermal stability and FT-IR analysis of Phosphonium-based deep eutectic solvents with different hydrogen bond donors, *J. Mol. Liq.*, 2017, **242**, 395–403.
26 L. Meneses, F. Santos, A. R. Gameiro, A. Paiva and A. R. C. Duarte, Preparation of binary and ternary deep eutectic systems, *J. Visualized Exp.*, 2019, **2019**, 1–5.
27 P. A. Frey and W. W. Cleland, Are there strong hydrogen bonds in aqueous solutions?, *Bioorg. Chem.*, 1998, **26**, 175–192.
28 M. J. Roldán-Ruiz, R. J. Jiménez-Riobóo, M. C. Gutiérrez, M. L. Ferrer and F. del Monte, Brillouin and NMR spectroscopic studies of aqueous dilutions of malicine: Determining the dilution range for transition from a "water-in-DES" system to a "DES-in-water" one, *J. Mol. Liq.*, 2019, **284**, 175–181.
29 H. T. Do, Y. Z. Chua, J. Habicht, M. Klinksiek, M. Hallermann, D. Zaitsau, C. Schick and C. Held, Melting properties of peptides and their solubility in water. Part 1: Dipeptides based on glycine or alanine, *RSC Adv.*, 2019, **9**, 32722–32734.
30 Y. Z. Chua, H. T. Do, C. Schick, D. Zaitsau and C. Held, New experimental melting properties as access for predicting amino-acid solubility, *RSC Adv.*, 2018, **8**, 6365–6372.
31 G. W. H. Höhne, H. K. Cammenga, W. Eysel, E. Gmelin and W. Hemminger, The temperature calibration of scanning calorimeters, *Thermochim. Acta*, 1990, **160**, 1–12.
32 A. Toda, M. Hikosaka and K. Yamada, Superheating of the melting kinetics in polymer crystals: A possible nucleation mechanism, *Polymer*, 2002, **43**, 1667–1679.
33 P. Cebe, D. Thomas, J. Merfeld, B. P. Partlow, D. L. Kaplan, R. G. Alamo, A. Wurm, E. Zhuravlev and C. Schick, Heat of fusion of polymer crystals by fast scanning calorimetry, *Polymer*, 2017, **126**, 240–247.
34 X. Hu, W. K. Raja, B. An, O. Tokareva, P. Cebe and D. L. Kaplan, Stability of silk and collagen protein materials in space, *Sci. Rep.*, 2013, **3**, 3428.
35 C. Held, T. Neuhaus and G. Sadowski, Compatible solutes: Thermodynamic properties and biological impact of ectoines and prolines, *Biophys. Chem.*, 2010, **152**, 28–39.
36 L. Fernandez, L. P. Silva, M. A. R. Martins, O. Ferreira, J. Ortega, S. P. Pinho and J. A. P. Coutinho, Indirect assessment of the fusion properties of choline chloride from solid-liquid equilibria data, *Fluid Phase Equilib.*, 2017, **448**, 9–14.
37 V. Meltzer and E. Pincu, Thermodynamic study of binary mixture of citric acid and tartaric acid, *Cent. Eur. J. Chem.*, 2012, **10**, 1584–1589.
38 C. Held, L. F. Cameretti and G. Sadowski, Measuring and Modeling Activity Coefficients in Aqueous Amino-Acid Solutions, *Ind. Eng. Chem. Res.*, 2011, **50**, 131–141.
39 L. Lange, K. Lehmkemper and G. Sadowski, Predicting the aqueous solubility of pharmaceutical cocrystals as a function of pH and temperature, *Cryst. Growth Des.*, 2016, **16**, 2726–2740.
40 L. Lange, M. Schleinitz and G. Sadowski, Predicting the Effect of pH on Stability and Solubility of Polymorphs, Hydrates, and Cocrystals, *Cryst. Growth Des.*, 2016, **16**, 4136–4147.
41 K. Wysoczanska, E. A. MacEdo, G. Sadowski and C. Held, Solubility Enhancement of Vitamins in Water in the Presence of Covitamins: Measurements and ePC-SAFT Predictions, *Ind. Eng. Chem. Res.*, 2019, **58**, 21761–21771.
42 *CRC Handbook of Chemistry and Physics*, ed. D. R. Lide, CRC Press LLC, Bosa Roca, United States, 82nd edn, 2001, p. 1.
43 I. M. Weiss, C. Muth, R. Drumm and H. O. K. Kirchner, Thermal decomposition of the amino acids glycine, cysteine, aspartic acid, asparagine, glutamic acid, glutamine, arginine and histidine, *BMC Biophys.*, 2018, **11**, 1–15.
44 R. C. Wilhoit and D. Shiao, Thermochemistry of Biologically Important Compounds. Heats of Combustion of Solid Organic Acids, *J. Chem. Eng. Data*, 1964, **9**, 595–599.
45 X. Meng, K. Ballerat-Busserolles, P. Husson and J.-M. Andanson, Impact of water on the melting temperature of urea + choline chloride deep eutectic solvent, *New J. Chem.*, 2016, **40**, 4492–4499.
46 J. P. Amend and H. C. Helgeson, Solubilities of the common L-α-amino acids as a function of temperature and solution pH, *Pure Appl. Chem.*, 1997, **69**, 935–942.
47 A. Apelblat and E. Manzurola, Solubility of oxalic, malonic, succinic, adipic, maleic, malic, citric, and tartaric acids in water from 278.15 to 338.15 K, *J. Chem. Thermodyn.*, 1987, **19**, 317–320.
48 H. Yang and J. H. Wang, Solubilities of 3-Carboxy-3-hydroxypentanedioic acid in Ethanol, Butan-1-ol, Water, Acetone, and Methylbenzene, *J. Chem. Eng. Data*, 2011, **56**, 1449–1451.
49 I. G. R. Gutz, *CurTiPot – pH and Acid–Base Titration Curves: Analysis and Simulation freeware, version 4.2*, http://www.iq.usp.br/gutz/Curtipot_.html.
50 A. Alhadid, L. Mokrushina and M. Minceva, Modeling of Solid–Liquid Equilibria in Deep Eutectic Solvents: A Parameter Study, *Molecules*, 2019, **24**, 1–19.
51 Merck, IR Spectrum Table & Chart, https://www.sigmaaldrich.com/technical-documents/articles/biology/ir-spectrum-table.html, (accessed 23 July 2020).
52 T. Mallik and T. Kar, Growth and characterization of non-linear optical L-arginine dihydrate single crystals, *J. Cryst. Growth*, 2005, **285**, 178–182.
53 S. Gowri, J. Sathiyabama and S. Rajendran, Corrosion inhibition effect of carbon steel in sea water by L-Arginine-Zn2+ system, *Int. J. Chem. Eng.*, 2014, **11**, 1–9.
54 A. M. Petrosyan and R. P. Sukiasyan, Vibrational spectra of L-arginine nitrates, *J. Mol. Struct.*, 2008, **874**, 51–56.
55 P. Mikes, A. Brož, A. Sinica, N. Asatiani and L. Bacakova, In vitro and in vivo testing of nanofibrous membranes doped with alaptide and L-arginine for wound treatment, *Biomed. Mater.*, 2020, 1–26.
56 P. Pimpang, R. Sumang and S. Choopun, Effect of concentration of citric acid on size and optical properties of

fluorescence graphene quantum dots prepared by tuning carbonization degree, *Chiang Mai J. Sci.*, 2018, **45**, 2005–2014.

57 L. C. Bichara, H. E. Lans, E. G. Ferrer, M. B. Gramajo and S. A. Brandán, Vibrational study and force field of the citric acid dimer based on the SQM methodology, *Adv. Phys. Chem.*, 2011, **2011**, 1–10.

58 N. T. Thuy and D. Le Minh, Size effect on the structural and magnetic properties of nanosized perovskite $LaFeO_3$ prepared by different methods, *Adv. Mater. Sci. Eng.*, 2012, **2012**, 1–6.

59 G. G. Stokes, Volume the Ninth, *Trans. Cambridge Philos. Soc.*, 1856, **9**, 5.

60 A. Einstein, Zur Theorie der Brownschen Bewegung, *Ann. Phys.*, 1906, **324**, 371–381.

61 P. Debye, *Polar Molecules*, Dover Publications, New York, USA, 1929.

62 G. H. Koenderink, H. Zhang, D. G. A. L. Aarts, M. P. Lettinga, A. P. Philipse and G. Nägele, On the validity of Stokes–Einstein–Debye relations for rotational diffusion in colloidal suspensions, *Faraday Discuss.*, 2003, **123**, 335–354.

63 J. L. Dote, D. Kivelson and R. N. Schwartz, A molecular quasi-hydrodynamic free-space model for molecular rotational relaxation in liquids, *J. Phys. Chem.*, 1981, **85**, 2169–2180.

64 L. Zhang and M. L. Greenfield, Rotational relaxation times of individual compounds within simulations of molecular asphalt models, *J. Chem. Phys.*, 2010, **132**, 184502.

65 S. K. Mann, T. N. Pham, L. L. McQueen, J. R. Lewandowski and S. P. Brown, Revealing Intermolecular Hydrogen Bonding Structure and Dynamics in a Deep Eutectic Pharmaceutical by Magic-Angle Spinning NMR Spectroscopy, *Mol. Pharmaceutics*, 2020, **17**, 622–631.

66 L. F. Zubeir, C. Held, G. Sadowski and M. C. Kroon, PC-SAFT modeling of CO2 solubilities in deep eutectic solvents, *J. Phys. Chem. B*, 2016, **120**, 2300–2310.

67 L. F. Cameretti and G. Sadowski, Modeling of aqueous amino acid and polypeptide solutions with PC-SAFT, *Chem. Eng. Process.*, 2008, **47**, 1018–1025.